Influence of homogenization on the microstructure, mechanical properties and texture of the twin-roll cast AA8006 sheet processed by accumulative roll-bonding

Miroslav Karlík[1,2*], *Petr* Homola[2,3], *Peter* Sláma[4], *Jiří* Čapek[5], and *Petr* Harcuba[1]

[1]Charles University, Faculty of Mathematics and Physics, Department of Physics of Materials, Ke Karlovu 5, 121 16 Prague 2, Czech Republic
[2]Czech Technical University in Prague, Faculty of Nuclear Sciences and Physical Engineering, Department of Materials, Trojanova 13, 120 00 Prague 2, Czech Republic
[3]Czech Aerospace Research Centre, Beranových 130, 199 05 Prague 9 – Letňany, Czech Republic
[4]COMTES FHT a.s., Průmyslová 995, 334 41 Dobřany, Czech Republic
[5]Czech Technical University in Prague, Faculty of Nuclear Sciences and Physical Engineering, Department of Solid-State Engineering, Trojanova 13, 120 00 Prague 2, Czech Republic

Abstract. Unhomogenized and homogenized AA8006 (Al-Fe-Mn-Si) alloy sheets twin-roll cast to strip 8.5 mm thick, processed by accumulative roll-bonding (ARB) on 2 mm thick sheets up to 6 cycles were studied. The microstructure was characterized by means of scanning and transmission electron microscopy and electron backscattered diffraction (EBSD), mechanical properties were monitored by hardness measurements and tensile tests. The macroscopic texture was determined by X-ray diffraction. The initial texture of the unhomogenized sheet is rotated cubic {001}<110> combined with recrystallization R texture {011}<211>, while the homogenized sheet has a cubic texture {001}<100> with remaining rolling component C {112}<111>. One ARB cycle leads to the formation of low-angle grain boundaries (LAGB) in original coarser grains and to a low angle rotation of the subgrains bounded by LAGB. After the 3rd and 6th ARB cycle unhomogenized and homogenized sheets show a common rolling texture of cold-rolled aluminium. The thermal stability of sheets processed by 6 ARB cycles was tested by isochronal annealing for 30 min up to 450°C. The homogenized sheet starts to recrystallize at 250°C, while the fine grain structure of the unhomogenized sheet is thermally stable up to 400°C.

1 Introduction

Accumulative Roll-Bonding (ARB) is a technique of grain refinement by severe plastic deformation (SPD) proposed by Saito *et al.* [1]. One ARB cycle consists in sheet cutting, surface treatment, stacking of two pieces, heating (optional), and rolling with 50% reduction in thickness. Since the sheet thickness remains unchanged by this cycle, ARB processing can be repeated as many times as desired, and an extremely high plastic strain is imposed on the material, resulting in structural refinement and increase of strength. ARB does not require any special equipment as other SPD methods such as equal channel angular pressing (ECAP) [2], high pressure torsion (HPT) [3], or cyclic extrusion and compression (CEC) [4], but only a conventional rolling mill. ARB processing has been applied to various metallic materials [5], and it has also been used for creating ultrafine grained metallic composites [6,7]. Ingot cast aluminium alloys are often used as starting materials for ARB [8-10]. An energy efficient technology of twin-roll casting (TRC) is known to produce materials with fine particles and small grain size, which are good starting materials to further grain refinement by ARB processing. Due to a rapid solidification of the metal, TRC sheets have a refined microstructure characterized by a finer dispersion of intermetallic particles and a higher level of matrix supersaturation with respect to the conventional ingot-cast materials [11]. Homogenization annealing reduces the differences between the surface layer and the core of the TRC strip and allows the precipitation of excess solute elements from the matrix [12] resulting in an improvement of the sheet ductility and workability [13,14]. A substantial grain refinement by ARB could be also accompanied by dissolution and reprecipitation of second phase particles [8,15]. Thus, it can have a similar effect as homogenization. A study of the homogenization and ARB processing on the microstructure, texture and mechanical properties of a commercial TRC AA8006 alloy is presented.

2 Experimental details

An AA8006 alloy containing (wt.%) 1.51 Fe, 0.40 Mn, and 0.16 Si was commercially twin-roll cast to an

* Corresponding author: Miroslav.Karlik@fjfi.cvut.cz

8.5 mm thick strip. The unhomogenized material was directly cold rolled down to 2 mm thickness. The second sample was cold rolled to 5.4 mm, homogenized at 610 °C for 18 h and further cold rolled to 2 mm. Unhomogenized and homogenized sheets were then recrystallization annealed for 30 min at 450 °C. One ARB cycle involved five steps: i) degreasing in tetrachloroethylene and brushing with stainless steel 0.3 mm wire brush, ii) stacking of two sheets of 300 mm × 50 mm × 2 mm in dimensions, iii) joining by Al wires to prevent sliding, iv) rolling at ambient temperature with 50% reduction in thickness without lubricant (roll diameter of 340 mm and peripheral speed of 30 m/min), v) trimming and smoothing of specimen edges in order to prevent the propagation of edge cracks. ARB processing was carried out up to 6 cycles. The microstructure of the samples was examined using a FEI Quanta 200 FEG scanning electron microscope (SEM) equipped with EDAX Trident electron backscattered diffraction (EBSD) system. Samples for EBSD were prepared by mechanical grinding and electrolytical polishing (at 12 °C, and 25 V) using Struers Lectropol 5 device filled with the solution of 5% perchloric acid in methanol. Transmission electron microscopy (TEM) samples were prepared by slow diamond blade cutting of slices in long transverse (LT) direction, mechanical grinding to 0.15 mm, punching, and twin-jet electrolytic polishing (at -30 °C, 30 V) in Struers Tenupol 2 unit filled with 6% perchloric acid solution in methanol. A JEOL JEM 2000FX microscope equipped with an energy dispersive spectrometer Bruker and CCD camera Veleta was used for observations of the thin foils at 200 kV accelerating voltage. The macroscopic texture in the sheet centre was determined by X-ray diffraction. The X'Pert PRO MPD diffractometer with cobalt radiation was used to the RX sample surface analysed by X-ray diffraction (XRD). Texture analysis was performed based on orientation distribution function calculation from experimental pole figures (with step size 5×5°), which were obtained on three diffraction lines {220}, {311}, {222} of aluminium phase. The pole figures were corrected for defocusing effect and background intensity. The evolution of mechanical properties after ARB processing was examined by HV10 hardness measurements and tensile test (samples 8 mm wide and 20 mm in gauge length, initial strain rate of 8.3×10^{-4} s^{-1}).

3 Results

3.1 Initial materials

3.1.1 Grains and particles

The grain structure and particle distribution of the sheets in the initial recrystallized condition are presented in Fig. 1. The grains of the unhomogenized sheet are heavily elongated in the rolling direction (Fig. 1a), their mean size in the normal (vertical) direction is 28.5 μm. Furthermore, the grains are not uniform, very coarse ones are present close to the surface and also in the volume. This grain character is accompanied by a higher amount of alloying additions in the solid solution and a non-uniform distribution of dispersoids (Fig. 1c,e). The majority of α-Al(Fe,Mn)Si and Al_6(Fe,Mn) particles is smaller than 500 nm (Fig. 1c), many Al_6(Fe,Mn) precipitates smaller than 100 nm are visible on the TEM micrograph (Fig. 1e). On the other hand, the homogenized sheet presents a quite uniform grain structure with nearly equiaxed grains, having in average 7.8 μm in the normal and 11.6 μm in the rolling direction, respectively (Fig. 1b). Also, the dispersoid particles are coarser (over 500 nm) and quite uniformly distributed (Fig. 1d,f), and the fine precipitate is absent (Fig. 1f).

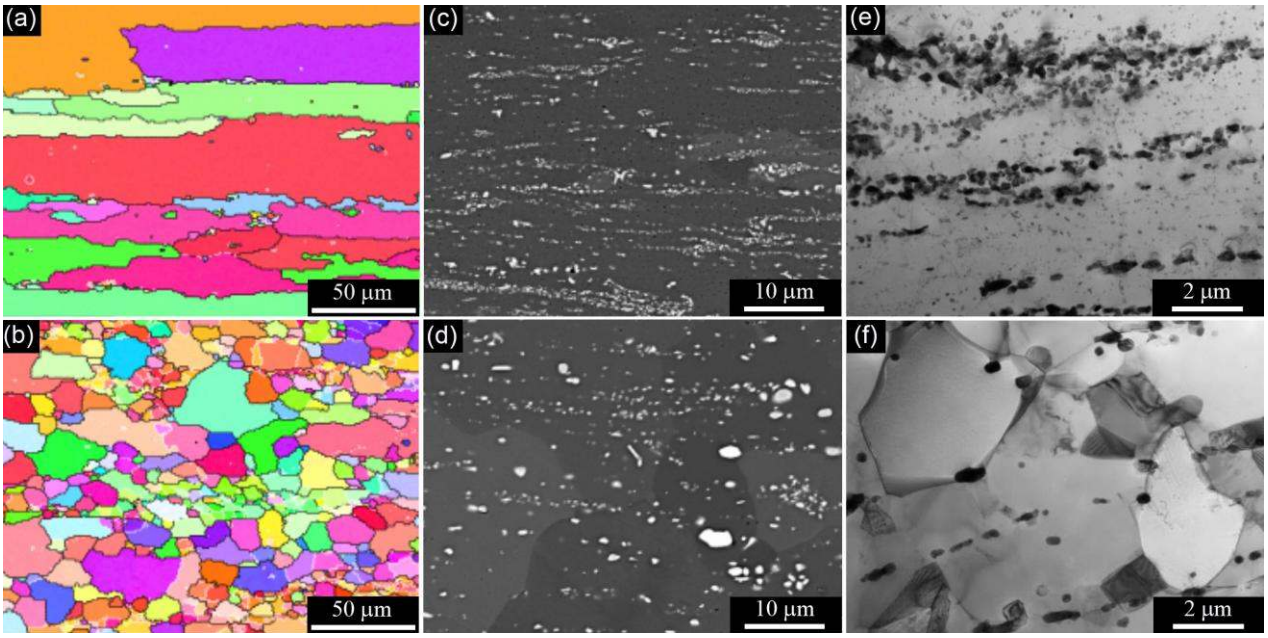

Fig. 1. Grain structure and particle distribution in unhomogenized (top) and homogenized sheet (bottom): (a,b) EBSD orientation maps, (c,d) SEM micrographs in the BSE signal, (e,f) TEM micrographs.

3.1.2 Texture

Fig. 2 shows orientation distribution functions (ODF) in selected Euler´s space sections (φ_2 values of 0° (90°), 45°, and 65°). The initial texture of the unhomogenized sheet is rotated cubic {001}<110> combined with recrystallization R texture {123}<634> (Fig. 2a), while the homogenized sheet has a cubic texture {001}<100> with remaining rolling component C {112}<111> (Fig. 2b).

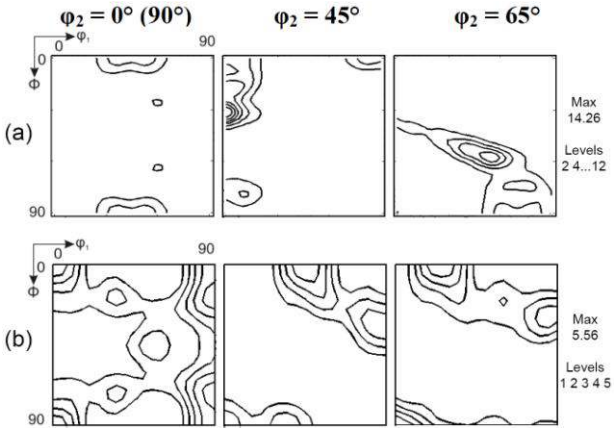

Fig. 2. ODF of the unhomogenized (a) and homogenized (b) sheets in the initial recrystallized condition (Euler´s space sections for φ_2 values of 0° (90°), 45°, and 65°).

3.2 ARB processed sheets

3.2.1 Mechanical properties

The unhomogenized initial material has higher strength and hardness and lower ductility (Fig. 3) than the homogenized one due to finer dispersion of primary and secondary phase particles (Fig 1) and also somewhat higher level of solute atoms in the matrix (electrical conductivity 29.7 MSm^{-1} and 30.7 MSm^{-1} for unhomogenized and homogenized sheet, respectively, measured by Foerster Sigmatest). For both variants of the initial materials, ARB processing causes the most important increase in strength and decrease of the elongation only during the first cycle (Fig. 3). In the following cycles, the changes are only moderate. Both materials show a small increase of the ultimate tensile strength (UTS) and also a surprising increase of elongation A_{20mm} after the 1st ARB cycle. When comparing the hardness values, there is a noticeable difference after the processing by 2 to 4 ARB cycles, where the unhomogenized sheets exhibit higher values of hardness. After the 5th and 6th ARB cycle the hardness of the unhomogenized sheet slightly decreases and approaches to the value of the homogenized one, while the tensile properties of the unhomogenized and homogenized sheets are practically identical.

3.2.2 Grains and subgrains

EBSD orientation maps showing the evolution of the grain structure of the sheets during ARB processing are

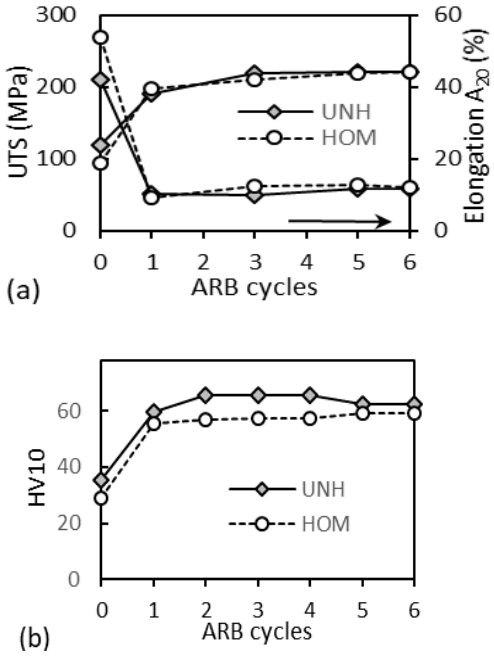

Fig. 3. Evolution of mechanical properties for unhomogenized and homogenized AA8006 sheets ARB processed at ambient temperature: (a) ultimate tensile strength (UTS), elongation A_{20mm}; (b) hardness HV10.

in Fig. 4. A gradual refinement of the grain size takes place in both materials. In the samples processed with a lower strain, i.e. after the first two ARB cycles (Fig. 4a,d), the deformed grains are separated by low-angle grain boundaries (LAGB) into subgrains. The LAGB are mostly inclined about 35° with respect to the rolling direction (RD). With increasing number of ARB cycles (increasing strain) the grain boundaries rotate to be parallel with RD and a lamellar grain structure is developed. In the homogenized sheet, the lamellar structure is observed already after the 3rd ARB cycle (Fig. 4e), while in the unhomogenized material there are still inclined shear bands in large areas of the original grains (Fig. 4b). After processing by 6 ARB cycles, both unhomogenized and homogenized sheets present a very fine and homogeneous grain structure (the grain size is about 0.3 μm in the normal direction - ND).

Transformation of LAGB to HAGB with increasing strain is evident from the plots in Fig. 5 indicating quantified results from another representation of EBSD orientation maps in Fig. 4. In this representation of EBSD grain boundary maps (not shown here), the boundaries are marked by different colours according to three ranges of mutual misorientation angles of adjacent grains in three categories: i) LAGB 2 to 5°, LAGB 5 to 15°, and HAGB > 15° and then treated by image analysis. From Fig. 5c it follows that in the initial recrystallized condition, the majority of grain boundaries are HAGB (unhomogenized sheet 90%, homogenized one 70%) During the first two ARB cycles, many LAGB are formed (Fig. 5a,b), and their percentage (addition of values from Fig. 5a and 5b) rises up to 66%. The corresponding fraction of HAGB is low and starting

* Corresponding author: Miroslav.Karlik@fjfi.cvut.cz

from the third ARB cycle it increases up to 71.5% and 83.8% for unhomogenized and homogenized sheet after 6 cycles, respectively. The curve for homogenized sheet is much steeper than for the unhomogenized one.

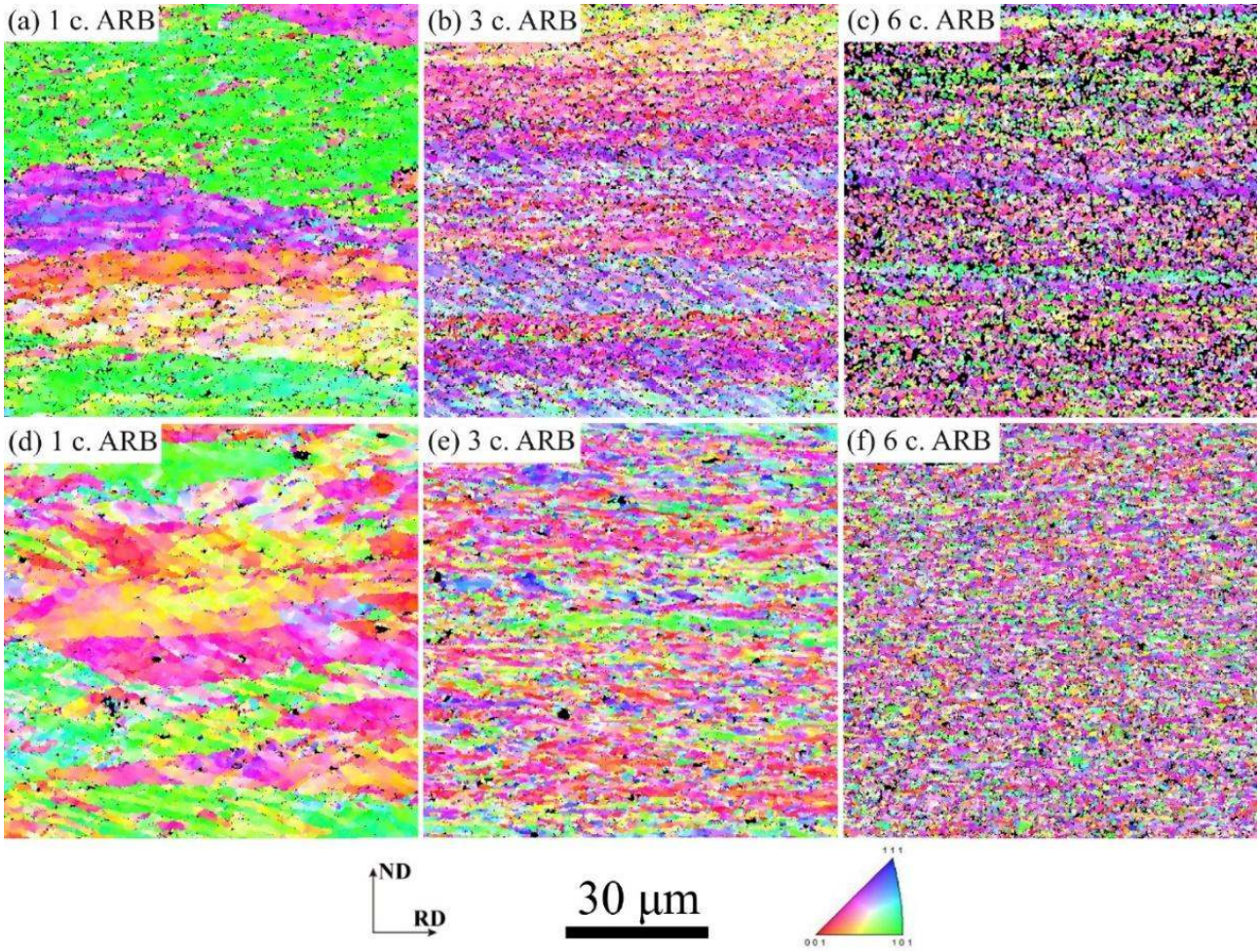

Fig. 4. EBSD orientation maps showing the evolution of the grain structure in the unhomogenized (a,b,c), and homogenized (e,f,g) sheets of the AA8006 alloy.

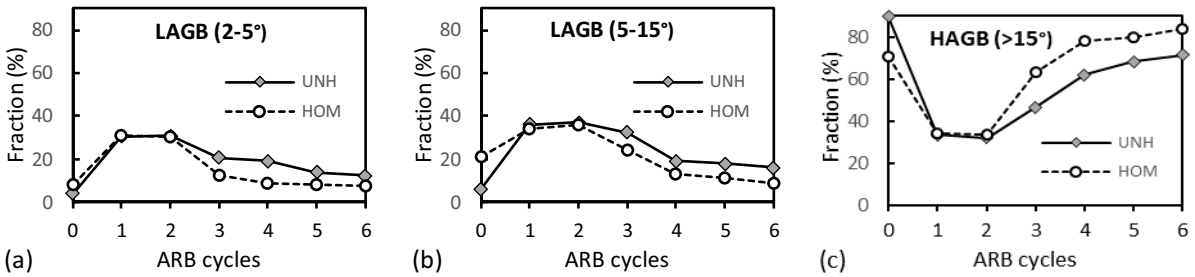

Fig. 5. Evolution of the fraction of low- and high-angle (sub)grain boundaries during ARB processing.

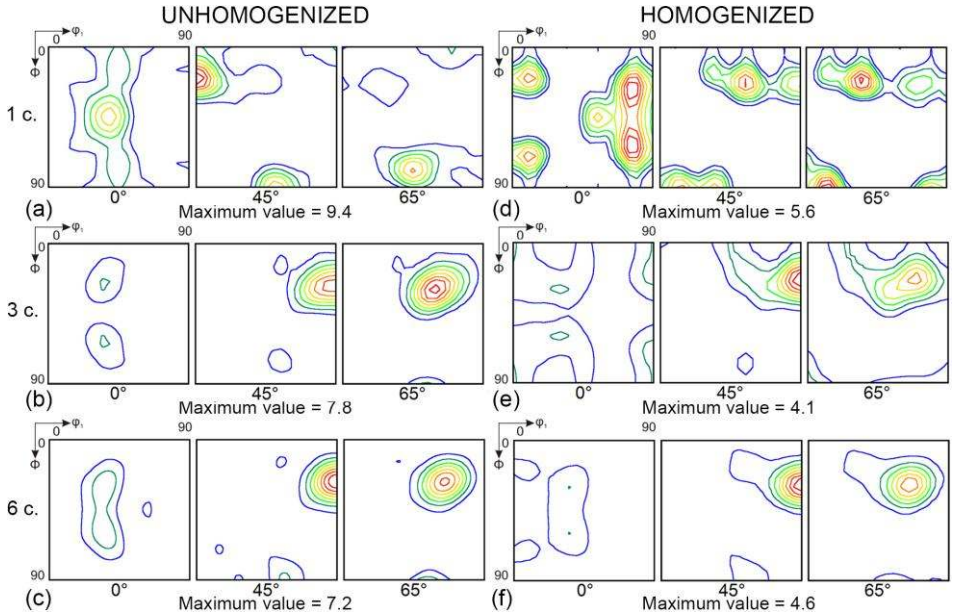

Fig. 6. Comparison of the ODF of the unhomogenized (a,b,c) and homogenized (d,e,f) sheets during ARB processing by 1, 3, and 6 cycles (Euler´s space sections for φ_2 values of 0° (90°), 45°, and 65°).

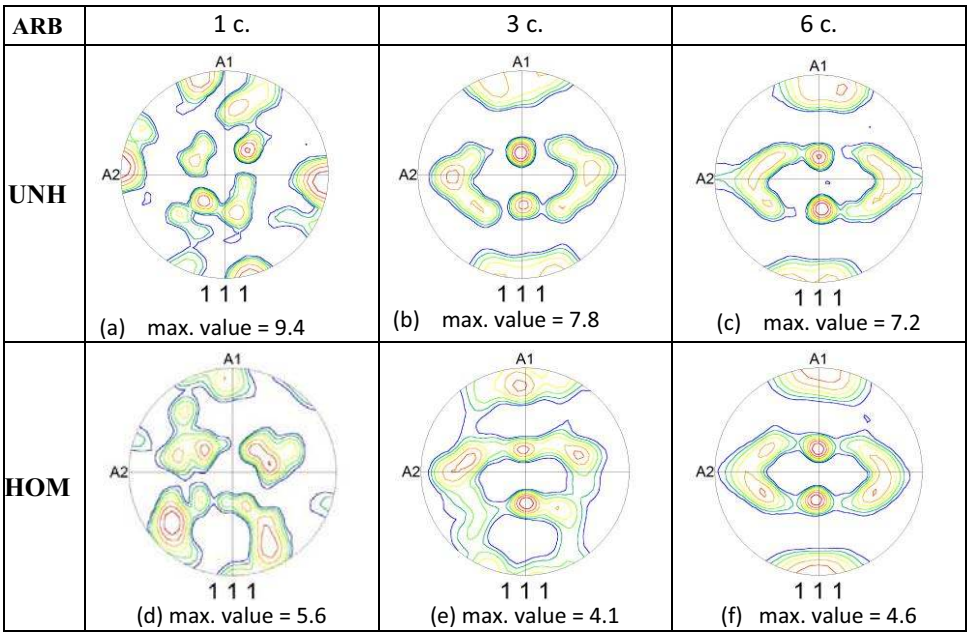

Fig. 7. Evolution of the pole figures (PF) of the unhomogenized (a,b,c) and homogenized (d,e,f) sheets during ARB processing by 1, 3, and 6 cycles.

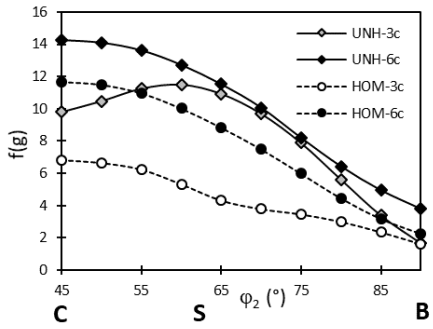

Fig. 8. Evolution of the β-fibre texture components during ARB processing.

3.2.3 Texture during ARB processing

As indicated above, the first ARB processing cycle results in the formation of the low-angle grain boundaries (LAGB) in the original large grains and in small changes in the orientation of subgrains delimited by LAGB. From the point of view of the texture only a rotation of the initial texture takes place in both unhomogenized and homogenized sheets, as it can be seen from the ODF in Fig. 6 and pole figures in Fig. 7. After 3 and 6 ARB cycles the texture corresponds more to a rolling texture of aluminium, with texture components along the β-fibre (Fig. 8). Typical components of the rolling texture, starting from the Cu texture C {112}<111>, through S texture {123}<634> to brass texture B {011}<211>. The component C is the strongest, the S texture prevails only in the unhomogenized sheet after the 3rd ARB cycle. From the β-fibre intensity (Fig. 8) and the maximum values of the ODF (Fig. 6) and the pole figures (Fig. 7) it follows that the unhomogenized sheets present a more pronounced texture that the homogenized ones. After 6 ARB cycles, the texture of the unhomogenized and homogenized sheet is very similar (Fig. 6,c,f, Fig. 7c,f, Fig. 8).

3.2.4 Thermal stability

The thermal stability of unhomogenized and homogenized sheets ARB processed up to 6 cycles was evaluated by an isochronal 30 min (1.8 ks) annealing at temperatures ranging from 50 to 450 °C. The softening behaviour was monitored by hardness measurements and the grain structure was examined by EBSD. From Fig. 9 it follows, that the hardness of both materials has practically the same course up to 200°C. Then at 250°C it drops for the homogenized sheet. From the EBSD maps it is evident that the grain structure of the unhomogenized sheet at 300°C is still deformed, while the homogenized material is already fully recrystallized. The hardness of the unhomogenized sheet decreases only moderately up to the temperature of 400°C. After annealing at 450°C, both materials are fully recrystallized and their hardness values are much closer than in the range from 250 to 400°C. However, the grains of the unhomogenized sheet are very large and not uniform (an abnormal grain growth took place - Fig. 9). On the other hand, the recrystallized homogenized ARB processed sheet shows a much more uniform and finer grain structure.

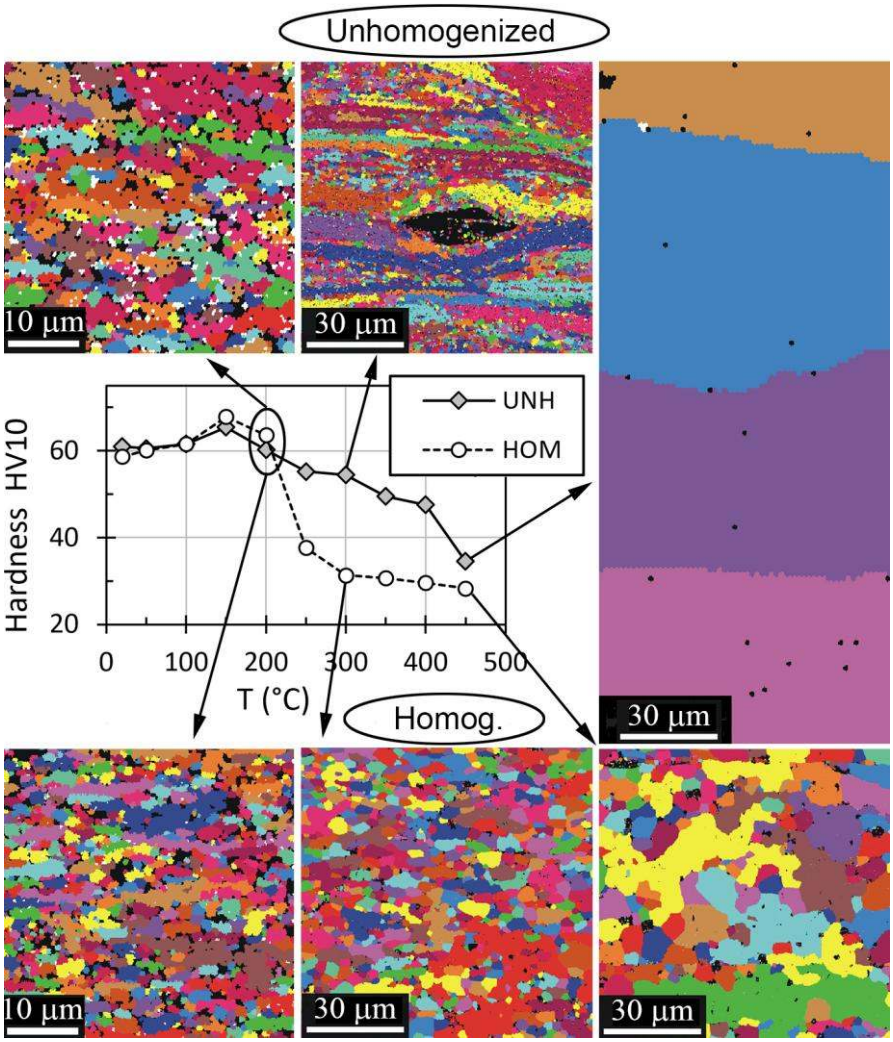

Fig. 9. Thermal stability of the unhomogenized and homogenized AA 8006 alloy sheets processed by 6 ARB cycles (during isochronal annealing for 30 min up to 450°C).

* Corresponding author: Miroslav.Karlik@fjfi.cvut.cz

4 Discussion

4.1 General microstructural features

As expected, ARB processing led to a substantial grain refinement from 28.5 μm and 7.8 μm in normal direction in the case of the unhomogenized and homogenized sheet, respectively (Fig. 1) up to 0.3 μm in the normal direction for both materials (Fig. 4). A similar grain refinement after 6 ARB cycles was achieved also for AA6063 and AA2014 alloy [16], AA5086 alloy [9], or AA3003 alloy [17]. The grain refinement is faster in the homogenized alloy (Fig. 4b,e), accompanied by a higher fraction of HAGB formed after 3 ARB cycles and further (Fig. 5c). After 6 ARB cycles, the grain structure of both materials is very similar (Fig. 4c,f).

4.2 Texture evolution

The textures of the initial materials are different: a rotated cubic {001}<110> combined with recrystallization R texture {123}<634> in the case of the unhomogenized sheet (Fig. 2a), and a cubic texture {001}<100> with remaining rolling component C {112}<111> for the homogenized one (Fig. 2b). However, ARB processing by 3 and more cycles (Figs. 6 and 7) leads to the development of a rolling texture of aluminium, with texture components along the β-fibre (Fig. 8). During ARB processing, the shear texture involving {001}<110> and {111}<110> orientations developed at the surface of the sheet due to the shear deformation induced by a large friction between the rolls and the sheet [18] is progressively introduced to the volume of the sheet. Thus, the final texture in the ARB sheet was mainly composed of Cu texture {112}<111>, through S texture (123)<634> to brass texture B {011}<211>. A similar texture evolution was found also for other Al alloys [8-10, 16-17]. These textural changes during the ARB process contributed to the formation of HAGB. After 6 ARB cycles, the texture of the unhomogenized and homogenized sheet is very similar (Fig. 6,c,f, Fig. 7c,f, Fig. 8). The unhomogenized sheets present only a more pronounced texture that the homogenized ones.

4.3 Mechanical properties

The most important increase in strength and decrease of the elongation during the first ARB cycle was expected. It is typical for ARB processing of many Al based materials [8-10, 16-17]. On the other hand, a slight increase of ductility during next ARB cycles involving higher equivalent strain is somewhat surprising. It was not observed for AA1000 sheet (pure Al) [19], a similar increase was found in the case of the AA8011 (Al-Fe-Si) alloy [8]. Kim et al. [15] explain this behavior by the enhancing of the recovery due to the presence of second phase particles. Our AA8006 alloy contains also numerous particles and so this is probably the reason for the slight increase of ductility after the first ARB cycle.

4.4 Thermal stability

The softening behaviour of the homogenized AA8006 sheet processed by 6 ARB cycles, i.e. the onset of recrystallization at 250°C is similar to the results reported for the same homogenized alloy in [20] after 3 and 5 ARB cycles. Birol [21] also reported that homogenized TRC Al-Fe-Mn sheet starts to recrystallize at much lower temperature (250 – 280°C) than the supersaturated unhomogenized one (400 – 450°C) [14]. Our ARB processed unhomogenized sheets behave in a similar way. However, their recrystallized grains are very large and not uniform due to abnormal grain growth took place (Fig. 9).

5 Conclusions

Unhomogenized and homogenized AAA8006 sheets were processed by accumulative roll-bonding (ARB) at ambient temperature. The main results of their characterization are summarized as follows:

i) ARB processing of both initial materials leads to a significant grain refinement. A homogeneous submicron (0.3 μm) grain size separated by more than 70% fraction of HAGB was achieved after 6 ARB cycles. The grain refinement is faster in the homogenized alloy.

ii) Even if the textures of the initial materials are different: a rotated cubic {001}<110> combined with recrystallization R texture {123}<634> in the case of the unhomogenized sheet, and a cubic texture {001}<100> with remaining rolling component C {112}<111> for the homogenized one, ARB processing by 3 and more cycles leads to the development of a rolling texture of aluminium, with common C,S,B texture components along the β-fibre.

iii) ARB processing causes the most important increase in strength and decrease of the elongation only during the first cycle. In the following cycles, the changes are only moderate. A slight increase of ductility during next ARB cycles is caused by an enhanced recovery due to the presence of second phase particles.

iv) The thermal stability of sheets processed by 6 ARB cycles was tested by isochronal annealing for 30 min up to 450°C. The homogenized sheet starts to recrystallize at 250°C, while the fine grain structure of the unhomogenized sheet is thermally stable up to 400°C.

This research was financially supported by ERDF in the frame of the project "Nanomaterials centre for advanced applications", No. CZ.02.1.01/0.0/0.0/15_003/0000485.

* Corresponding author: Miroslav.Karlik@fjfi.cvut.cz

References

1. Y. Saito, H. Utsunomiya, N. Tsuji, T. Sakai, Acta Mater. **47**, 579-583 (1999)
2. R.Z. Valiev, T.G. Langdon, Prog. Mater. Sci. **51**, 881-981 (2006)
3. R.Z. Valiev, R.K. Islamgaliev, I.V. Alexandrov, Prog. Mater. Sci. **45**, 103-189 (2000)
4. M. Richert, Q. Liu, N. Hansen, Mater. Sci. Eng. A **260**, 275-283 (1999)
5. N. Tsuji, In: Altan, B.S. (Ed.), Severe Plastic Deformation, Toward Bulk Production of Nanostructured Materials, Nova Science Publishers, New York, 545–565 (2005)
6. K. Wu, H. Chang, E. Maawad, W.M. Gan, H.G. Brokmeier, M.Y. Zheng, Mater. Sci. Eng. A **527**, 3073-3078 (2010)
7. P. Qu, L. Zhou, H. Xu, V.L. Acoff, Metall. Mater. Trans. A **45**, 6217-6230 (2014)
8. H.W. Kim, S.B. Kang, N. Tsuji, Y. Minamino, Metall. Mater. Trans. A **36**, 3151-3163 (2005)
9. S. Roy, D. Satyaveer Singh, S. Suwas, S. Kumar, K. Chattopadhyay, Mater. Sci. Eng. A **528**, 8469-8478 (2011)
10. H. Xie, M.P. Wang, W. Chen, Y. Jia, J. Mater. Eng. Perform. **25**, 1199-1210 (2016)
11. S. Sarkar, M.A. Wells, W.J. Poole, Mater. Sci. Eng. A, **421**, 276 (2006)
12. M. Slámová, P. Sláma, M. Cieslar, Mater. Sci. Forum **519–521**, 365 (2006)
13. I. Peter, M. Rosso, In: ICAA13, Ed: H. Weiland, A. D. Rollett, W. A. Cassada, TMS (The Minerals, Metals & Materials Society). 177-182 (2012)
14. Y. Birol, Scr. Mater. **60**, 5-8 (2009)
15. H.W. Kim, S.B. Kang, N. Tsuji, Y. Minamino, Acta Mater.**53**, 1737-1749 (2005)
16. V.G. Arigela, J. Scharnweber, L. Lisenhoeft, P. Chekonin, R. Schaarschuch, S.K. Kolli, N.R. Palukuri, J. Rengaswamy, W. Skrotzki, Kovove Mater. **53**, 245-249 (2015)
17. H. Pirgazi, A. Akbarzadeh, R. Petrov, J. Sidor, L. Kestens, Mater. Sci. Eng. A **492**, 110-117 (2008)
18. C.H. Choi, J.W. Kwon, K.H. Oh, D.N. Lee, Acta Mater. **45**, 5119-5128 (1997)
19. H. Pirgazi, A. Akbarzadeh, R. Petrov, J. Sidor, L. Kestens, Mater. Sci. Eng. A **497**, 132-138 (2008)
20. M. Cieslar, M. Poková, Materials **7**, 8058-8069 (2014).
21. Y. Birol, Scr. Mater. **59**, 611-614 (2008)